

$\gamma\gamma$ scattering and extended vector dominance

U. Maor and E. Gotsman

Department of Physics and Astronomy, Tel Aviv University, Tel Aviv, Israel

(Received 28 December 1982)

We show that the extended vector-dominance model (EVDM) provides a reasonable fit to the presently available data, both for the photon-photon cross section $\sigma_{\gamma\gamma}$ and for the photon structure function F_2^γ for values of $Q^2 \lesssim 25 \text{ GeV}^2$. The EVDM approach allows us to circumvent the problem of double counting concerning the hadronic and pointlike pieces of the photon, and yields a value of $b_2 \approx -0.04$, for the undetermined coefficient of the second moment of F_2^γ .

I. INTRODUCTION

It has been recognized for some time now¹⁻³ that a study of the photon structure function provides a unique source of information for the gluonic corrections to the pointlike coupling of a photon to a quark-antiquark pair (see Fig. 1). Accordingly, the measurement of the photon structure function in $\gamma\gamma$ reactions provides a unique test of QCD. Indeed, recent measurements⁴⁻⁶ of F_2^γ include a comprehensive comparison between data and QCD predictions. There is, however, a certain ambiguity in $\gamma\gamma$ reactions analysis which stems from the fact that the photon serves simultaneously both as a target and as a probe. We can therefore analyze the $\gamma\gamma$ interaction either by means of the target variables x and Q^2 and the photon structure function $F_2^\gamma(x, Q^2)$, or by means of the probe variables Q^2 , and W and the cross section $\sigma_{\gamma\gamma}(Q^2, W)$. These two descriptions are connected through the relations

$$F_2^\gamma(x, Q^2) = \frac{Q^2}{4\pi^2\alpha} \sigma_{\gamma\gamma}(Q^2, W), \tag{1}$$

$$W^2 = Q^2 \left[\frac{1-x}{x} \right]. \tag{2}$$

In other words, a complete description of $\gamma\gamma$ data in terms of $\sigma_{\gamma\gamma}(Q^2, W)$ leaves no degrees of freedom for the study of $F_2^\gamma(x, Q^2)$ and vice versa.

In this paper we have examined in detail the extended vector-dominance model^{7,8} (EVDM) predictions for $\gamma\gamma$ reactions. Our aim was to investigate the uniqueness of QCD fits presented in the experimental data analysis,⁴⁻⁶ as well as an attempt to study the obvious dual role played by target and probe photons. In Sec. II we present the model and its results for $\sigma_{\gamma\gamma}(Q^2, W)$. In Sec. III we study the photon structure function F_2^γ and some kinematical constraints. The interplay between target and probe is further discussed in Sec. IV and our conclusions are summa-

rized in Sec. V.

II. THE MODEL

The basic assumption of the EVDM is that a photon couples to the hadronic current through its direct (coherent) coupling, to an infinite number of vector mesons for which one assumes a Veneziano-type linear mass spectrum,

$$m_n^2 = m_0^2(1 + \lambda n) \tag{3}$$

with direct photon-vector couplings which satisfy the relation

$$\frac{m_n^2}{f_n^2} = \frac{m_0^2}{f_0^2}. \tag{4}$$

The standard value of $\lambda=2$ is determined^{7,8} from $Q^2=0$ photoproduction analysis. The predictions of the model are in good agreement with photoproduction, pion-form-factor, and deep-inelastic ep data.^{7,8}

In the context of $\gamma\gamma$ reactions we first apply the EVDM to the virtual (probe) photon and obtain

$$\begin{aligned} \sigma_{\gamma\gamma}(Q^2, W) &= \sum_{n=0}^{\infty} \left[\frac{e}{f_n} \right]^2 \left[\frac{m_n^2}{m_n^2 + Q^2} \right]^2 \sigma_{n\gamma}(W) \\ &= \left[\frac{e}{f_0} \right]^2 \sigma_{0\gamma}(W) \sum_{n=0}^{\infty} \left[\frac{m_n^2}{m_n^2 + Q^2} \right]^2 \frac{\sigma_{n\gamma}(W)}{\sigma_{0\gamma}(W)}, \end{aligned} \tag{5}$$

where $\sigma_{n\gamma}(W)$ denotes the $Q^2=0$ cross section of the n th vector meson with the real (target) photon. $\sigma_{0\gamma}(W)$ can also be expressed in terms of the EVDM, however, this will not change our analysis as $(e/f_0)^2 \sigma_{0\gamma}(W) = \sigma_{\gamma\gamma}(W)$. This also avoids the need to specify f_0^2 , which has been determined in other investigations.^{7,8}

In evaluating Eq. (5) we need to specify $\sigma_{n\gamma}$, for which we use a Regge relation

$$\frac{\sigma_{n\gamma}(W)}{\sigma_{0\gamma}(W)} = \left(\frac{m_0^2}{m_n^2} \right)^\alpha. \tag{6}$$

We proceed and carry out a dual analysis with both a diffractive (Pomeron) term, taking $\alpha=1$, and a Regge term with $\alpha=\frac{1}{2}$. This is consistent with our assumed form for the real $\gamma\gamma$ cross section which is parametrized⁹:

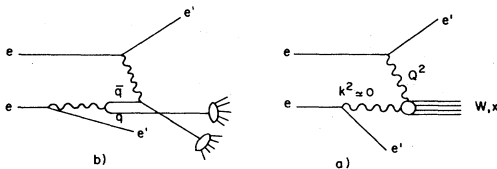


FIG. 1. $\gamma\gamma$ reactions as extracted from $ee \rightarrow eex$. (a) General notation and kinematics. (b) The pointlike sector in a $\gamma\gamma$ reaction.

$$\sigma_{\gamma\gamma}(W) = \sigma_{\gamma\gamma}^D + \sigma_{\gamma\gamma}^R = 240 + \frac{270}{W} \quad (7)$$

(σ in nb, W in GeV) so as to satisfy factorization and Regge behavior. This leads to

$$\sigma_{\gamma\gamma}^D(Q^2, W) = \sigma_{\gamma\gamma}^D(W) \sum_{n=0}^{\infty} \frac{1}{(1 + \lambda n + Q^2/m_0^2)^2}, \quad (8)$$

$$\sigma_{\gamma\gamma}^R(Q^2, W) = \sigma_{\gamma\gamma}^R(W) \sum_{n=0}^{\infty} \frac{(1 + \lambda n)^{1/2}}{(1 + \lambda n + Q^2/m_0^2)^2}. \quad (9)$$

These two equations form the basis of our analysis.

The sums given in (8) and (9) can be expressed in terms of the generalized Reimann ζ functions. For the purpose of this study we have evaluated these sums numerically. However, some insight can be gained by observing their asymptotic values for $Q^2 = \infty$; with $\lambda = 2$ we get

$$F^D(Q^2) = \sum_{n=0}^{\infty} \frac{1}{(1 + \lambda n + Q^2/m_0^2)^2} \rightarrow \frac{1}{2} \frac{m_0^2}{m_0^2 + Q^2}, \quad (10)$$

$$F^R(Q^2) = \sum_{n=0}^{\infty} \frac{(1 + \lambda n)^{1/2}}{(1 + \lambda n + Q^2/m_0^2)^2} \rightarrow \frac{\pi}{4} \left[\frac{m_0^2}{m_0^2 + Q^2} \right]^{1/2}. \quad (11)$$

For completeness we have evaluated (8) and (9) with the ω and ϕ families added to the ρ assuming the standard 3:1: $-\sqrt{2}$ SU(3) coupling-constant ratios.

The first result emanating from this EVDM study is a suggested modification of the real $\gamma\gamma$ cross-section parametrization (7). A straightforward calculation at $Q^2 = 0$ yields a 23% increase of $\sigma_{\gamma\gamma}^D(W)$ and 69% increase of $\sigma_{\gamma\gamma}^R(W)$; i.e., we suggest the parametrization

$$\sigma_{\gamma\gamma}(W) = 295 + \frac{460}{W} \quad (7')$$

(σ in nb, W in GeV). This implies a stronger threshold enhancement of $\sigma_{\gamma\gamma}(W)$ than suggested by (7) and is indeed compatible with the data and the constraints imposed by factorization.¹⁰

Our main goal is to study the Q^2 dependence of $\sigma_{\gamma\gamma}(Q^2, W)$. Our results are shown in Fig. 2 compared to the PLUTO experimental data⁴ with $3.5 < W_{\text{vis}} < 10$ GeV. The calculated Q^2 dependence (solid curve) was averaged accordingly using Eq. (7'). The PLUTO data shows sharp departure from standard vector-dominance-model VDM predictions at $Q^2 \geq 1$ GeV². This has been attributed⁴ to the pointlike nature of the photon. Our calculation contains two terms. One is the Regge term (9) which decreases with increasing W and has a wider Q^2 distribution than the Pomeron contribution [see (10) and (11)]. Our analysis thus suggests that the observed flattening of the Q^2 dependence, observed experimentally, is stronger at low energies, where the $\sigma_{\gamma\gamma}^R$ term is more important. The prediction at high energy where $\sigma_{\gamma\gamma} = \sigma_{\gamma\gamma}^D$ is displayed in Fig. 2 by the dashed curve.

We can conclude from the above that the EVDM provides a satisfactory description of the Q^2 dependence of $\sigma_{\gamma\gamma}(Q^2, W)$. This result does not relate at all to the question of the role played by the pointlike versus the hadronic

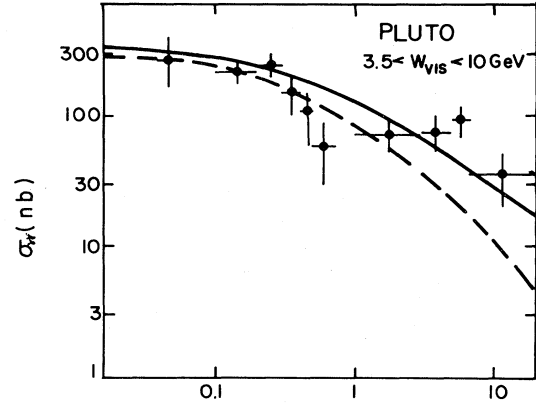


FIG. 2. PLUTO (Ref. 4) total $\gamma\gamma$ cross section as a function of Q^2 . Solid curve indicates the EVDM prediction for $W < 10$ GeV. Dashed curve denotes the high-energy limit of the EVDM prediction. (See text).

pieces of the photon, as our summation over an infinity of vector mesons means that we sum over both photon sectors. The relations between the pointlike and hadronic photon pieces will be discussed in Sec. IV.

III. THE PHOTON STRUCTURE FUNCTION

The model presented in Sec. II is essentially a description for the virtual probing photon. However, as we have already noted, the kinematics of $\gamma\gamma$ reactions as expressed in Eqs. (1) and (2) does not leave any degree of freedom, once $\sigma_{\gamma\gamma}(Q^2, W)$ has been specified. We now proceed to investigate the consequence of our model when expressed in terms of the target variable x .

We have compared our calculations with the published results on $F_2^{\gamma}(x, Q^2)$ coming from the PLUTO (Ref. 4), CELLO (Ref. 5), and JADE (Ref. 6) experiments. There is an important kinematical observation which we wish to stress. Experimental studies of $\sigma_{\gamma\gamma}(W)$ as well as $\sigma_{\gamma\gamma}(W, Q^2)$ show⁹ a strong cross-section enhancement at W values as low as 1.0–1.5 GeV which we shall denote as W_m . For low energies, when $W < W_m$, the cross section

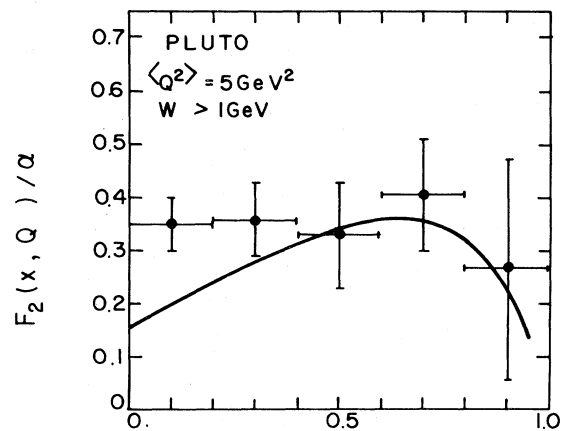


FIG. 3. PLUTO (Ref. 4) photon structure function with $\langle Q^2 \rangle = 5$ GeV². Solid curve is our calculation averaging over $1 < Q^2 < 10$ GeV².

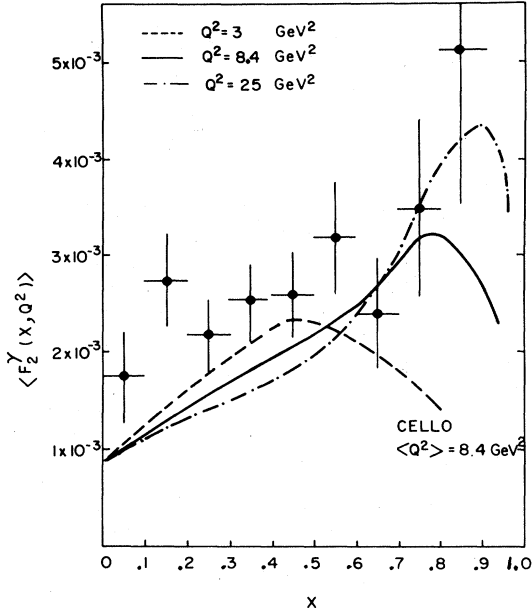


FIG. 4. CELLO (Ref. 5) photon structure function with $\langle Q^2 \rangle = 8.4 \text{ GeV}^2$. Our calculations are given at values of $Q^2 = 3, 8.4, \text{ and } 25 \text{ GeV}^2$.

drops rapidly to zero at threshold.¹¹ Since W , Q^2 , and x are connected through Eq. (2), when we evaluate $F_2^\gamma(x, Q^2)$ its shape should reflect the shape of $\sigma_{\gamma\gamma}(Q^2, W)$ rescaled according to Eq. (2). In a model of this type, where a direct relation exists between $F_2^\gamma(x, Q^2)$ and $\sigma_{\gamma\gamma}(W)$, F_2^γ must decrease very rapidly for $x < Q^2/(Q^2 + W_m^2)$ and vanish as $x \rightarrow 1$, as expected from general arguments. This kinematical observation is very important for the actual analysis of the three experiments⁴⁻⁶ which have averaged their results over a wide Q^2 range.

Figure 3 shows our averaged results compared with the PLUTO data.⁴ Figure 4 shows the CELLO data⁵ and our calculations at different Q^2 values. The changing shape of F_2^γ as a function of Q^2 is clearly seen. Figure 5 shows the data of JADE (Ref. 6) and our results. There is some am-

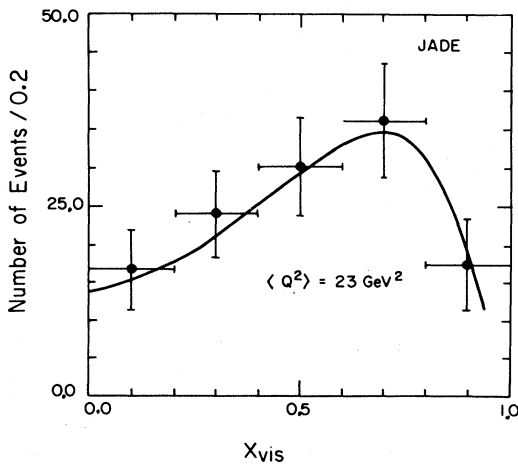


FIG. 5. JADE (Ref. 6) photon structure function with $\langle Q^2 \rangle = 23 \text{ GeV}^2$. Fitted line was normalized to data. (See text.)

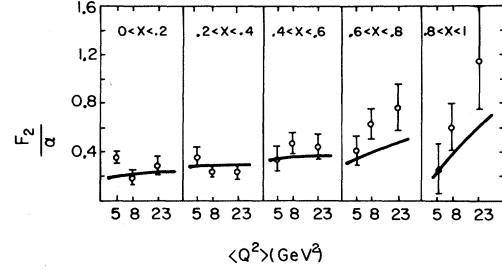


FIG. 6. x dependence of photon structure function. Data (Ref. 12) compared with our calculations.

biguity concerning the normalization of our graph in Fig. 5. The data has been presented in arbitrary units and we have normalized our calculations according to the published information on $\langle F_2^\gamma \rangle$ which is given in normalized units. Our normalization may therefore be off by as much as 25%.

The published $F_2^\gamma(x, Q^2)$ data have been compared with QCD, with and without VDM contributions. It is evident from our study that such fits are not conclusive. Furthermore, it has been claimed^{4,6} that the Q^2 dependence of $\langle F_2^\gamma \rangle$ shows a $\log Q^2$ behavior as expected from QCD. Indeed, a strong Q^2 dependence is observed at low $Q^2 < 5 \text{ GeV}^2$. We believe that this Q^2 behavior reflects the kinematics rather than the dynamics of $\gamma\gamma$ reactions. At low Q^2 a sizable sector of the x scale corresponds to $x < Q^2/(Q^2 + W_m^2)$. This sector, for which F_2^γ decreases, is longer for smaller Q^2 . All in all we get a strong Q^2 dependence of $\langle F_2^\gamma \rangle$, which reflects this kinematical phenomena. This is demonstrated in Fig. 6 where the F_2^γ data has been divided into several x intervals. The kinematics of $\gamma\gamma$ reactions implies strong Q^2 variations at high x as observed; not surprisingly our calculations reproduced this feature.

We have noted the strong variations of F_2^γ as a function of Q^2 . This phenomenon occurs mainly at low and medium values of Q^2 . At high Q^2 our F_2^γ calculations scale (modulo $\log Q^2$). Assuming that $\sigma_{\gamma\gamma}(W) = a + b/W$, we expect

$$F_2^\gamma(x, Q^2) = \frac{Q^2}{4\pi^2\alpha} \left[aF^D(Q^2) + \frac{b}{W}F^R(Q^2) \right]. \quad (12)$$

Substituting the asymptotic values of $F^D(Q^2)$, and $F^R(Q^2)$, Eqs. (10) and (11), we obtain

$$F_2^\gamma(x, Q^2) = A + B \left[\frac{x}{1-x} \right]^{1/2}, \quad (13)$$

where A and B are directly related to a and b . Equation (13) is valid for $x < Q^2/(Q^2 + W_m^2)$. In general Eq. (13) holds modulo some unknown threshold function which ensures that F_2^γ vanishes as $x \rightarrow 1$. Assuming that this threshold function is linear in $1-x$ leads to

$$F_2^\gamma(x, Q^2) = A(1-x) + B\sqrt{x(1-x)}. \quad (14)$$

It should be noted that we still have the freedom to introduce additional $\log Q^2$ dependences. An important ingredient of the EVDM is the Regge assumption which can be modified so that

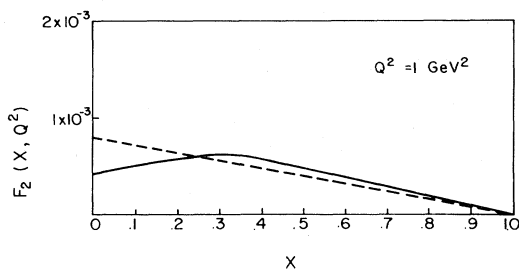


FIG. 7. Photon structure function calculated at $Q^2=1 \text{ GeV}^2$. Dashed line is VDM prediction of Ref. 13.

$$\sigma_{\gamma\gamma} = \left[a + \frac{b}{W} \right] \ln \left[\frac{W^2}{\Lambda^2} \right]; \quad (15)$$

this would introduce a $\log W$ dependence into $F_2^\gamma(x, Q^2)$. This point will be amplified in Sec. IV.

IV. DISCUSSION

The distinction between the hadronic and pointlike pieces of the photon has been frequently discussed in the literature.^{1-3,13} It is known that a low- Q^2 probe should "observe" the photon as a hadronic object; on the other hand, as $Q^2 \rightarrow \infty$ the photon structure function should be dominated by the pointlike gluon-corrected piece. However, the transition from hadronic to pointlike descriptions is not obvious. We do not know if the hadronic-photon sector vanishes as $Q^2 \rightarrow \infty$, or whether it scales as a background to F_2^γ . From this point of view there is some advantage to EVDM studies where the distinction between the hadronic and pointlike sectors is not made and we are able to calculate parameters which are undetermined in the standard QCD calculations.^{2,3,13}

We start with a consistency check. Peterson, Walsh, and Zerwas¹³ estimate the hadronic contribution to F_2^γ from the analysis of $\pi^- p \rightarrow \mu^+ \mu^- x$. According to this VDM point of view for the target photon, one obtains a scaled background contribution to F_2^γ ;

$$F_2^{\gamma, \text{had}}(x, Q^2) = \left[\frac{e}{f_\rho} \right]^2 F_2^\pi(x) = \frac{\pi\alpha}{f_\rho^2} (1-x). \quad (16)$$

$$M_2^\gamma(Q^2) = \frac{1}{4\pi^2\alpha} \int_0^1 dx \left[\frac{1}{2} a m_0^2 + \frac{\pi m_0 b}{4} \left(\frac{x}{1-x} \right)^{1/2} \left[\ln \left(\frac{Q^2}{\Lambda^2} \right) + \ln \left(\frac{1-x}{x} \right) \right] \right]. \quad (19)$$

Equation (19) holds for $x < Q^2/(Q^2 + W_m^2)$ and can be evaluated analytically.

We take $m_0 = \frac{9}{12} m_\rho + \frac{1}{12} m_\omega + \frac{2}{12} m_\phi$ and obtain $a_2 = 0.403$; this is quite compatible with QCD calculations.^{2,3} Furthermore, we note that $F^D(Q^2)$ and $F^R(Q^2)$ converge to their asymptotic values only at exceedingly high Q^2 . Using numerical values of $F^D(Q^2)$ and $F^R(Q^2)$ calculated for $Q^2 = 20 \text{ GeV}^2$, we obtain $a_2 \simeq 0.6$. Similarly, we realize a value of $b_2 = -0.031$ for $Q^2 \rightarrow \infty$ and $b_2 \simeq -0.04$ at $Q^2 = 20 \text{ GeV}^2$. This last result indicates a small, but nonvanishing, hadronic-photon piece which persists even in the limit of $Q^2 \rightarrow \infty$. The actual value of

We have calculated $F_2^{\gamma, \text{had}}$ using the probe variable Q^2 . We note that experimentally the data⁴ are consistent with VDM for $Q^2 \leq 1 \text{ GeV}^2$, namely, the probe itself behaves as a hadron. Once we assume that the probe is described by VDM, we can calculate F_2^γ derived from such an input. This is shown in Fig. 7 where our $F_2^{\gamma, \text{VDM}}$ is calculated at $Q^2 = 1 \text{ GeV}^2$ and compared with $F_2^{\gamma, \text{VDM}}$ suggested in Ref. 13. The two functions are very similar except at very small values of x . The main difference between the two approaches is that $F_2^{\gamma, \text{VDM}}$ calculated by assuming VDM for the probe vanishes as $Q^2 \rightarrow \infty$. The hadronic-target-photon piece, if it exists as $Q^2 \rightarrow \infty$, is hidden in such a model in the EVDM output.

Technically, we may formulate the problem as follows. The quark and gluon distributions in a target photon are given by the Altarelli-Parisi moments equations,¹⁴ the solution of which is a combination of a homogeneous solution and a particular solution of the inhomogeneous equation. Peterson, Walsh and Zerwas¹³ associate the homogeneous solution with VDM and estimate it phenomenologically. The same problem is discussed in Refs. 2 and 3. Given the F_2^γ moments parametrization

$$M_n^\gamma(Q^2) = \int_0^1 dx x^{n-2} F_2^\gamma(x, Q^2) \\ = a_n \ln \left[\frac{Q^2}{\Lambda^2} \right] + b_n, \quad (17)$$

one can calculate all coefficients from QCD except b_2 , which remains a free parameter.

The advantage of our model is that the second moment of F_2^γ can be readily calculated. We start with Eqs. (12) and (15):

$$F_2^\gamma(x, Q^2) = \frac{Q^2}{4\pi^2\alpha} \left[a F^D(Q^2) + \frac{b}{W} F^R(Q^2) \right] \\ \times \ln \left[\frac{W^2}{\Lambda^2} \right], \quad (18)$$

and using the asymptotic Q^2 limits for $F^D(Q^2)$ and $F^R(Q^2)$, Eqs. (10) and (11), we obtain, on substituting in Eq. (17)

b_2 obtained is compatible with the free parameter used in Ref. 3.

V. CONCLUSIONS

The main conclusion of this investigation is that $e\gamma$ deep-inelastic scattering may be described by either probe or target variables. Our study shows that presently available data^{4,6} on $\sigma(Q^2, W)$, $F_2^\gamma(x, Q^2)$, and its first moment are described rather well by the EVDM. We conclude, thus, that QCD fits to F_2^γ which have been used in the data analysis⁴⁻⁶ are not unique. This observation calls for

some clarification especially concerning the compatibility of the EVDM with QCD.

(1) If one assumes that the (real) $\gamma\gamma$ total cross section grows logarithmically with energy, then a model such as utilized above automatically yields a structure function with a $\log Q^2$ behavior. There is, however, an intrinsic difference between this result, which is obtained in the EVDM only after appending the assumed $\log W$ dependence of $\sigma_{\gamma\gamma}$ and the $\log Q^2$ dependence of QCD where it is a fundamental ingredient of the theory.

(2) QCD, as well as our calculation, predict a maximum of $F_2^{\gamma}(x, Q^2)$ at high x , which is supported by the data.⁴⁻⁶ In QCD this maximum reflects the contribution of the quark box diagram, while in our calculation the connection is made between the high- x maxima of F_2^{γ} and the threshold enhancement of $\sigma_{\gamma\gamma}$. Once again we note that the model used in this paper serves as a tool which correlates the real $\gamma\gamma$ and deep-inelastic $e\gamma$ phenomena.

(3) As has already been noted, one expects the hadronic contribution to $F_2^{\gamma}(x, Q^2)$ to rise at small x and drop off at large x . What is not *a priori* clear is the Q^2 dependence of the hadronic contribution to F_2^{γ} , which is fixed by the b_2 term in the first moment of F_2^{γ} . Our calculation yields a value for b_2 , a quantity which is undetermined in QCD

studies. Since b_2 does not vanish as $Q^2 \rightarrow \infty$ we conclude that the hadronic sector of the photon target is not zero in the high- Q^2 limit.

(4) We wish to stress once more that the interest in the EVDM originates from its ability to successfully simulate the pointlike properties of the *target* photon by assuming that the *probe* photon can be approximated by an infinite series of increasingly heavier vector mesons. Attention should be drawn to the dual role in the description of $e\gamma$ deep-inelastic scattering played by the target and the probe.

(5) Finally we add that a great deal of the data available on F_2^{γ} has been collected at low and medium Q^2 where it is difficult to distinguish between kinematics and dynamics.

ACKNOWLEDGMENTS

This research was supported in part by the Fund for Basic Research Administered by the Israel Academy of Science and Humanities. The early part of this work was done while one of us (U.M.) was visiting the Theory Group at DESY. He wishes to thank Dr. T. Walsh and colleagues for their kind hospitality.

¹E. Witten, Nucl. Phys. **B120**, 189 (1977).

²W. A. Bardeen and A. J. Buras, Phys. Rev. D **20**, 166 (1979); **21**, 2041 (E) (1980).

³D. W. Duke and J. F. Owens, Phys. Rev. D **22**, 2280 (1980).

⁴PLUTO Collaboration, Ch. Berger *et al.*, Phys. Lett. **107B**, 168 (1981).

⁵CELLO Collaboration, H. J. Behrend *et al.*, Contributed paper, XXIst International Conference on High Energy Physics, Paris, 1982 (unpublished).

⁶JADE Collaboration, W. Bartel *et al.*, DESY Report No. 82-064, 1982 (unpublished).

⁷M. Greco, Nucl. Phys. **B63**, 398 (1973).

⁸*Electromagnetic Interactions of Hadrons*, edited by A. Donnachie and G. Shaw (Plenum, New York, 1978), Vol. 2.

⁹TASSO Collaboration, R. Brandelik *et al.*, Phys. Lett. **97B**, 448 (1980); PLUTO Collaboration, Ch. Berger *et al.*, *ibid.* **99B**, 287 (1981).

¹⁰G. Alexander, U. Maor, and P. G. Williams, Phys. Rev. D **26**, 1198 (1982).

¹¹The continuously decreasing cross-section distribution changes very close to threshold to describe resonance peaks and then vanishes below $W - 2m_{\pi}$. Such fine details are of no relevance in this context.

¹²Susan Cooper, DESY Report No. 82-050, 1982 (unpublished).

¹³C. Peterson, T. F. Walsh, and P. M. Zerwas, Nucl. Phys. **B174**, 424 (1980).

¹⁴G. Altarelli and G. Parisi, Nucl. Phys. **B126**, 298 (1977).